



Development of a community-scale autonomous water purifier (AWP) prototype to remove heavy metals

Dulce K. Becerra-Paniagua^{a*} • Joel Pantoja Enriquez^b • Araceli Hernández-Granados^c • Guillermo Ibáñez Duharte^b • Joel Moreira Acosta^c • P. J Sebastian^a

^aInstituto de Energías Renovables. Universidad Nacional Autónoma de México. Temixco, Morelos, México

^bUniversidad de Ciencias y Artes de Chiapas. Tuxtla Gutiérrez, Chiapas, México

^cInstituto de Ciencias Físicas. Universidad Nacional Autónoma de México. Cuernavaca, Morelos, México

^dUniversidad del Valle de México. Tuxtla Gutiérrez, Chiapas, México

Received 06 15 2021; accepted 12 29 2021

Available 06 30 2022

Abstract: In this paper, we present the design and evaluation of a prototype Autonomous Water Purifier (AWP) for removing heavy metals from contaminated water. The AWP prototype uses solar energy for its operation. An autonomous photovoltaic system was designed to operate up to 8 hours per day and to generate a water flow of 112 liters per day. The prototype was designed to remove biological and chemical agents. It was achieved the elimination of total coliforms, fecal coliforms, total alkalinity, total hardness, total solids, chloride and sulfate from 50 to 100%. It could also remove heavy metals. Pb^{2+} , Hg^{2+} , Cd^{2+} and Cu^{2+} were eliminated from 80 to 99%. This wide range of contaminant removal shows a unique way to treat contaminated water in comparison to existing purification systems. The prototype was evaluated with river and spring water from different rural communities of Chiapas, Mexico. The results indicate that the prototype can completely remove contaminants in natural waters and get water that meets the guidelines of the Mexican official standards. This work helps to solve problems in marginalized communities and natural disaster areas where there is no access to clean water, electricity and suffer from waterborne diseases.

Keywords: Hybrid solar system, Water purification, Water treatment, Heavy metal removal

*Corresponding author.

E-mail address: dkbp@ier.unam.mx (Dulce K. Becerra-Paniagua).

Peer Review under the responsibility of Universidad Nacional Autónoma de México.

1. Introduction

Nowadays, shortage of clean water in the world has become a big and serious problem since it affects thousands of people, especially the vulnerable population in rural and remote areas. This problem does not arise from the “lack of water” in the area, this comes from many other factors and even in areas with high water resources. For example, Latin America and the Caribbean (LAC) are regions with high water resources, they possess almost 34% of the fresh water in the world (Mekonnen et al., 2015). Nevertheless, access to potable and purified water is insufficient and their quality is inadequate (Flachsbarth et al., 2015). According to the World Health Organization (WHO) and the United Nations International Children's Emergency Fund (UNICEF), around 2.2 billion people around the world do not have safely managed drinking water services, 4.2 billion people do not have safely managed sanitation services, and 3 billion people lack basic handwashing facilities (World Health Organization & United Nations Children's Fund, 2015; 2019). The COVID-19 pandemic has woken up the previous red alerts.

It is well-known that lack of water brings many social problems. For example, in 2017 almost 1.6 million people died globally from diarrheal diseases (WHO & UNICEF, 2017a) and in Latin America and the Caribbean, it is the second leading cause of death (Pan American Health Organization, 2017). Diarrhea is completely preventable and treatable and the main causes come from the consumption of contaminated water mainly by *Escherichia coli* (*E. coli*) and heavy metals (Jaishankar et al., 2014), both are associated with toxicity and bioaccumulation in living beings (Marazzato et al., 2020; Shaharoon et al., 2019).

In the case of Latin America and the Caribbean, 74.3% and 31.3% of the population respectively have access to safely managed water and sanitation services (Pan American Health Organization & World Health Organization, 2019). Mexico is one of the Latin American countries with a larger supply of fresh water in the world, every year Mexico receives around 1,449,471 million cubic meters of water in the form of precipitation. The North, Center and Northwest regions possess 1/3rd of the renewable water with 4/5th of the population (1,581.28 m³/inhab/year) which is less than the Southeastern region with 2/3rd of the renewable water and 1/5th of the population (10, 718.25 m³/inhab/year) (PAHO & WHO, 2019). Even though, the Southeastern region possesses more water, this region is less developed in Mexico. The most affected states are Oaxaca, Guerrero, Campeche, and Chiapas. Among all these states, in 2016 the state of Chiapas had the highest renewable water resources per year and per capita in the country, 113,903 hm³/year and 21,419 m³/inhab/year, respectively (Statistics on Water in Mexico, 2017). Even with these resources of water most rural communities of this state

don't have access to clean water, electricity and suffer from water-borne diseases.

In order to find solutions for this type of problem, many reports have proved that household water treatment can be the most cost-effective option (Holtman et al., 2018; Murray et al., 2020). However, this method has a disadvantage, such as taste and poor disinfection efficiency. Other options are the use of solar radiation for drinking water treatment through SODIS (solar water disinfection) (Kohn et al., 2016; Parsa et al., 2020; Vivar et al., 2017) this method had confirmed efficiency to remove bacteria, fungi, and viruses. Nevertheless, the time needed for solar exposure is at least 6 hours; if it is cloudy this is up to 2-3 days (Wang et al., 2016).

Another potential method to improve the efficiency of solar disinfection has been reported by the addition of a photocatalyst, such as titanium dioxide (TiO₂) (Fernández-Ibáñez et al., 2015; Wu et al., 2014). Although TiO₂ increased the effectiveness of the SODIS, the suspension of TiO₂ nanoparticles had to be separated before human consumption (otherwise it could be a human health risk), also this process is costly and difficult. Even with this big potential, the SODIS is limited to the disinfection efficiency and the scale-up. This is because the large-scale systems such as the continuous flowing or pumping circulation both need electricity and they ceased to be useful for rural and remote areas that lack clean water and electricity.

Due to these reasons, other works have developed hybrid photocatalytic-photovoltaic prototypes to treat contaminated water (Qin et al., 2015; Vivar et al., 2012). Other researchers reported hybrid systems using solar radiation, these systems were pilot-scale solar photoreactors, which included flat plate reactors (FPRs) and compound parabolic collector (CPC) reactors (Ochoa-Gutiérrez et al., 2018; Wang et al., 2016). Many hybrid systems for remote locations have been developed to desalinate water through reverse osmosis (Alghoul et al., 2016; Peng et al., 2018) and ultrafiltration membranes (Clayton et al., 2019).

The main advantage of hybrid systems is that they do not require conventional energy for their operation. It favors their implementation in remote areas that lack clean water and electricity. However, despite its great functionality, each method has its disadvantages such as high cost, taste, laboratory scale, synthetic feeding water, low removal efficiency from toxic contaminants such as heavy metals (mercury, lead, arsenic, cadmium and copper). In addition, the experiments only showed few contaminants such as dyes, salts, microorganisms.

The aim of this work is to build and evaluate an autonomous water purifier (AWP) prototype, with practical and accessible dimensions/weight to make it easy to handle, highly efficient to remove heavy metals from remote locations, with the purpose of enhancing water quality in a community-scale.

Our results showed that the AWP prototype has an extensive range for the removal of contaminants in comparison to equivalent water treatment systems from the same locations, and the electricity generated by the solar cells can be used for running the whole system. The water performance, design, operational conditions, and photovoltaic system were studied.

2. Materials and methods

2.1 Design of the AWP prototype

2.1.1 Feed water quality

The design of purification steps in the AWP prototype is dependent on the feed water quality, therefore the chemical and microbiological contaminants commonly found in most surface water and groundwater of Latin America were identified (Table 1). Based on these results, it was possible to determine and select the stages convenient for the purification system and achieve suitable drinking water that met the guidelines by Mexican official standards for purified water.

Table 1. Main chemical and microbiological contaminants present in natural waters of Latin America (WHO & UNICEF, 2017b).

Contaminant type	
Microbiological	Concentration range
Total coliforms	2000-180,000
Fecal coliforms	MPN/100 mL
	1500-50,000
	MPN/100 mL
Chemical	Concentration range
Total alkalinity	200-600 mg/mL
Total hardness	150-700 mg/mL
Total solids	200 -900 mg/mL
Sulfate	10-50 mg/mL
Chloride	10-30 mg/mL
Heavy metals	Concentration range
Mercury (Hg ²⁺)	10-30 mg/L
Lead (Pb ²⁺)	10-50 mg/L
Arsenic (As ³⁺)	10-30 mg/L
Cadmium (Cd ²⁺)	10-30 mg/L
Copper (Cu ²⁺)	15-30 mg/L

2.1.2. Solar resources

Mexico is within the latitudes 15°N to 35°N, with annual average solar radiation levels of approximately 5.00 kWh/m²-year (Matsumoto et al., 2014). The northern region of the coastal zone of the Gulf of Mexico can reach a radiation up to 6.7 kWh/m²-day (Pérez-Denicia et al., 2017). While, the southeast region, including Chiapas, can reach a solar radiation level of up to 4.76 kWh/m²-day (REdataexplorer,

2022), and the annual average solar radiation at this area is 5.66 kW/m²-year (Valdes-Barrón et al., 2014).

2.1.3. Components of AWP prototype

The AWP prototype is integrated by: (1) photovoltaic panels (capture the energy of the incident solar radiation and convert it into electrical energy); (2) controllers (regulate the electric current that arrives at the batteries); (3) batteries (store the electrical energy), (4) inverters (convert the input of direct current to alternating current). The purification system is located inside the housing (26) of the AWP prototype.

To put the prototype to operate, first it is necessary to pre-treat the feed water in the storage tank (5); inside there are coagulants, flocculants and disinfectants dispenser (6). The fluid (27) is formed by a pressure pump (7) for forced flow, purification processes are integrated by adsorption columns (8 and 9) with polymeric materials (polypropylene and polyester), zeolite ion-exchange column (10) of heavy metals, adsorption columns with activated carbon materials (11 and 12), polymer resins ion exchange columns (13) of hardness, a transmembrane pressure pump (14), semipermeable membranes (15 to 18), adsorption column (19), ultraviolet lamp (20) and a pressurized storage tank (21).

A purified water taps (22) and a digital indicator display (23) are located on the front outer surface of the AWP prototype. A shut-off valve (24) for feed water is located on the lateral outer surface, on the lower outer surface is located the trailer (25) that provides mobility to the device. The external surface of the device is formed by a rigid structure (26) with high resistance to corrosion and wear.

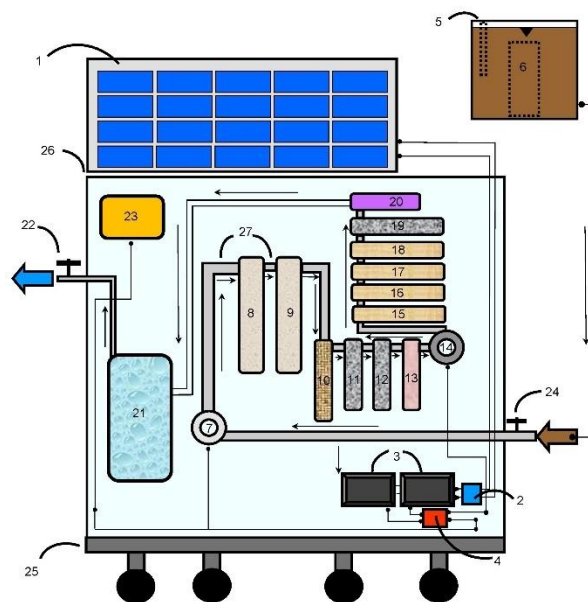


Figure 1. Technical schematic of AWP prototype.

2.2. Sizing and construction of AWP prototype

2.2.1. Dimensioning of the autonomous photovoltaic system

The purpose of photovoltaic dimensioning is to calculate system elements needed to reliably supply the electrical energy needed for a purification system to operate and achieve a completely autonomous system. The following environmental and operational parameters for calculations of the photovoltaic sizing were considered:

1. The daily power demand of the equipment required by the purifier was determined according to alternating (AC) and direct (DC) power consumption. It was obtained that the power demand required by the purifier is 52 W in AC, and for 8 working hours it is needed 416 Wh/d.
2. The solar peak time (SPT) and average SPT considered for Chiapas, México was 5.3 kWh/m² (Pérez-Denicia et al., 2017).
3. Backup time chosen was N=4 days. This means the time in which the solar panels will not capture solar energy due to unfavorable conditions and whole consumption will be met with energy stored in the batteries.
4. The number of panels was calculated from total actual consumption relation (E_T) and the peak power of panel (P_p), the result obtained was 90 Wp.
5. The battery capacity was calculated for a backup time of 4 days, and daily consumption of 468 Wh/d. Thus, it was obtained the necessity of 2 batteries of 115 Ah and 12 V for each one.
6. The capacity of the controller was calculated in order to obtain the maximum current (I_{max}) flowing in the installation. For this, it was calculated the current produced in the panel (I_p), the current consuming charges (I_c) and based on the maximum of these currents it was calculated the one supported by the controller (Luque & Hegedus, 2003).

2.2.2. AWP prototype construction

It was carried out the construction of the autonomous purifier based on the AWP prototype design (Figure 1). The material for manufacturing the prototype was galvanized steel of 24 caliber. Once it was built, we continued to integrate the purification system and the photovoltaic system. Two deep cycle batteries (115 A and 12 V) with a useful life of 5 years and one solar panel (90 W/m² power) the useful life of 20 years were connected to ensure that the equipment works correctly.

The autonomous photovoltaic system was constructed according to the dimensions as shown in Table 2.

It was observed that the energy generated satisfied the energy demand required by the AWP prototype for 8 hours of operation. The permeation rate from the membrane was 14 liters/hour (L/h), thus the working period of the prototype showed a total flow of 112 liters/day (L/day). This gives a

calculation of 56 persons water need per day (assuming that a person will consume only 2 L/day). If the water is required for personal hygiene, then the number of persons will decrease up to 3-4 (since the average quantity of water used for bathing per person is 20 L/d).

Table 2. Autonomous photovoltaic system sizing.

Photovoltaic parameters	Dimensions
Total power of the system:	52 W
Theoretical energy consumption for 8 hours:	416 Wh/d
Total actual consumption required by the purifier:	468 Wh/d
Peak power of solar panel:	90 W/m ²
Battery capacity (2 batteries):	115Ah, 12 V
Controller capacity:	10 A
Inverter capacity:	100 W

In Figure 2, we can see the final AWP prototype. The overall dimensions are: 110 cm x 90 cm x 70 cm (height x length x width) and possesses relatively low weight ≈70 kg.



Figure 2. Front and side view of the working AWP prototype.

2.3. Evaluation procedures

2.3.1. Study area

The study was carried out in Chiapas, Mexico (17°33'23.5" N and 93°22'51.7" O). The main reason was because Chiapas has the largest population without access to drinking water and occupies the first place of extreme poverty in the country (Gutiérrez-Jiménez, 2014). One of the ten leading causes of children's mortality in Chiapas is diarrheal illness from contaminated water (Stevens et al., 2008). For example, one rural community with the highest social backwardness and marginalization index is the municipality of Oxchuc, located in the region of Los Altos, Chiapas (16°43'00" N and 92°37'00" O), where around 70.85% of the households do not have safe drinking water supply (Gutiérrez-Jiménez et al., 2019).

2.3.2. Sampling

The surface water samples were collected from the Santo Domingo River located at Chiapa de Corzo, Mexico (16°42'30" N and 93°01'01" O), as far as possible from the riverbank, trying not to remove the ground and avoiding stagnant zones. The spring water samples were collected from Los Altos, Mexico (16°43'00" N and 92°37'00" O). Both samples were stored in drums of 60 and 50 liters to be filtered by the AWP prototype, also 2 liters of sterilized jars were kept for their microbiological and chemical analysis. Before storing the samples in the drums, they were washed three consecutive times and were also completely immersed in the opposite direction of the river's flow. Samples were kept in ice boxes during transfer and were processed after a maximum period of 2 h (Rice et al., 2017). The temperature, pH (HI 98129, Hanna Instruments), and turbidity (HI 93703C, Hanna Instruments) of the water samples were determined immediately on the spot before they arrived at the laboratory. Microbiological and chemical analyses were conducted on the water samples before and after the treatment with the filter from the AWP prototype. The water samples, how they look like (a) before and (b) after purification are shown in Figure 3.



Figure 3. (a) Natural raw water sample before purification and (b) clean water sample after purification.

2.3.3. Feed water pre-treatment

The pre-treatment process at the storage tank (Figure 1, subsection 5) consisted of a clarification and disinfection step before being filtered by the AWP prototype. The clarification treatment was performed by the Jar-test technique (Aragonés-Beltrán et al., 2009) to determine the optimum dose of coagulant and disinfectant for the dispenser (6) inside the storage tank. It was found that the optimum dose of the coagulant (10% v/v aluminum sulfate) was 1320 mL for the total volume of raw water (110 liters). After this calculation, it was measured the initial and final parameters such as turbidity and pH (Table 4), and the optimum dose used for the disinfectant was 20 mL for the same volume of raw water. By adding an excess of chlorine, it was reached free residual chlorine that acted as a disinfectant. The samples were left in contact with the disinfectant for 15 to 30 minutes. After that, the concentration of free residual chlorine was measured with

a digital Checker in order to achieve the right concentration of chlorine's residual content (1.5 mg/mL).

2.4. Analytical details

2.4.1 Total coliform and fecal coliform

The total number of coliforms was determined by the method of most probable number (MPN). The process consisted of inoculating 10, 1 and 0.1 mL of the raw water sample into Durham tubes, each volume was replicated into 5 tubes to give 15 tubes in total. Each Durham tube contained 10 mL of lauryl tryptose broth (LTB), and the gas production was used as an indicator of the presence of coliforms. The tubes were incubated at 35 °C for 48 hours (Erdem et al., 2004). It was compared the number of tubes giving a positive reaction to a standard chart and record the number of bacteria present in it (WHO, 1997). The results of the examination for the coliform group carried out by the multiple-tube fermentation technique are reported in terms of the most probable number (MPN/100 mL) of organisms present.

The presence of fecal coliforms was determined by performing the fecal coliform tests. The test consisted of the inoculation of *Escherichia coli* in broth tubes, introducing a loop with bacteria taken from the LBT and it was incubated at 44 °C for 24 hours. The presence of turbidity and gas formation after incubation was an indication of the presence of *E. coli* (Rice et al., 2017).

2.4.2. Turbidity, odor and taste

The Nephelometric method was used to determine the turbidity and color from the water samples. This method consisted of a comparison between the intensity of light scattered by the sample under defined conditions and the intensity of light scattered by a standard reference suspension under the same conditions, greater the dispersion of light higher the turbidity and color. The data were collected using a calibrated turbidimeter HACH TL2300 EPA with a reference suspension of formazin polymer prepared under specific conditions. The sensitivity of the instrument permits detecting turbidity range of 0 to 4000 NTU. The unit in which turbidity is expressed when it was been determined by the nephelometric method are Nephelometric Turbidity Unit (NTU) (Rice et al., 2017).

The test for determining the odor consisted of diluting a raw water sample with odor-free water to a dilution that has a minimal perceptible odor. It is taken as a fact that there is no absolute value for odor and that the test is used for comparison only (Rice et al., 2017).

2.4.4. Total alkalinity

The alkalinity in water was determined by titration technique. Phenolphthalein and methyl orange as indicator reagent were used. 100 mL of sample was transferred in a 250 mL Erlenmeyer flask and added a few drops of indicator reagent, until a slight coloration was noted. It was titrated with a standard solution of sulfuric acid (H₂SO₄, 0.02 N) until it turned

from pink to colorless. The volume of spent acid was determined. Few drops of the methyl orange indicator solution were added. The titration was continued with acid solution until turned yellow or orange. The volume of spent acid was determined (Rice et al., 2017).

2.4.5. Total hardness

Total hardness is defined as the sum of the calcium (Ca^{2+}) and magnesium (Mg^{2+}) ion concentrations, both expressed as calcium carbonate (CaCO_3) in milligrams per liter. The method to determine the total hardness consisted of an assessment using eriochrome T as visual indicator, which is red in the presence of calcium and magnesium and turns blue when these are complexed form or absent. A 50 mL sample of water was taken, 1 or 2 mL of H_2SO_4 buffer was added to achieve a pH of 10.0 and an amount (0.2 g) of the eriochrome T indicator was added. The sample became reddish in color. It was titrated with a 0.01 M Ethylenediaminetetraacetic acid (EDTA) solution, stirring continuously until the reddish hue disappeared. The last drops were added with intervals of 3 s to 5 s. At the end the sample changed from reddish to blue. The EDTAs spent on the titration in the sample are noted for later calculation (Rice et al., 2017).

2.4.6. Chloride and sulfate

The determination of chloride ions (Cl^-) consisted of a titration with silver nitrate using potassium chromate as an indicator. A 100 mL sample was used, the pH was adjusted between 7 and 10.1 mL of potassium chromate indicator solution was added, and it was titrated with the silver nitrate standard solution until it turned yellow to orange. The silver reacted with the chlorine to form a precipitate of white silver chloride.

For the determination of sulfate ions (SO_4^{2-}), a 100 mL sample of raw water was brought to capacity with deionized water to 100 mL and 20 mL of buffer reagent was added. The buffer reagent was a solution of magnesium chloride ($\text{MgCl}_2 \cdot 6\text{H}_2\text{O}$), sodium acetate ($\text{CH}_3\text{COONa} \cdot 3\text{H}_2\text{O}$), and acetic acid 99% (CH_3COOH) in 500 mL of distilled water. Then, 0.2 g of barium chloride crystals ($\text{BaCl}_2 \cdot 2\text{H}_2\text{O}$) was added and stirred for 1 min at constant speed. A sulfate ion mass concentration reference solution was prepared for the calibration curve of 147.9 mg anhydrous sodium sulfate in 1 liter of deionized water. A calibration curve was constructed with a minimum of 5 points in addition to blank, within the range of 0 mg/l to 40 mg/l of SO_4^{2-} . After stirring, it was emptied into a quartz cell and read the absorbance of the samples and the reference solutions at 420 nm in a cell of 1 cm using a Perkin Elmer Lambda 20 UV-Vis Spectrophotometer (Rice et al., 2017). The mass concentration of sulfate ions (SO_4^{2-}) was determined with the Beer-Lambert law.

2.4.7. Heavy metals

The ion exchange in aqueous solution on the zeolite columns (10) was studied for the heavy metals such as Pb^{2+} , Hg^{2+} , Cd^{2+} and Cu^{2+} . To do this, several zeolite samples (*clinoptilolite-K*) were washed using deionized water, then separated by settling. After that, were dried for 24 hours in an oven (*H-33 Riossa*) at 110 °C and kept in dry containers.

The exchange isotherm experimental data was obtained from the ion exchange column (10). The samples were filtered over this column. For this purpose, it was used a 500 mL solution prepared with an initial ion metal concentration of 10-100 mg/L.

Hydrochloric acid (HCl) was used to adjust the initial pH from 7 to 5, because it is reported that the maximum and optimum pH values for metal adsorption lie between 5 to 6.5 (Elboughdiri, 2020). The zeolite and the solution were left in contact until they reached the equilibrium (24 h). It was measured the absorbance of the final concentration of ions after being filtered by the AWP prototype using an Inductively Coupled Plasma Optical Emission Spectroscopy, ICP-OES (*Thermo Scientific iCAP 6000 SERIES*) spectrometer. The concentration was calculated also by the calibration curve method, this process was done by establishing the calibration curve over standard metal solutions at concentrations from 10 to 100 mg/L.

The metal cation removal percentage (%R) was calculated from the difference of initial (C_i) and final (C_f) metal cation concentration in each sample by the following equation (Erdem et al., 2004):

$$\%R = \frac{C_i - C_f}{C_i} \times 100 \quad (1)$$

3. Results and discussion

3.1. Microbiological water quality

The data shown labeled as initial concentration (C_i) means the results from the samples before receiving any treatment (*raw water*) and the final concentration (C_f) is the results of samples treated by the AWP prototype (*treated water*). The microbiological water quality assessment results are presented in Table 3, the average was calculated from 3 times of sampling.

The C_i coliform values obtained from river and spring water were $54,000 \pm 3\%$ and $79 \pm 2\%$ MPN/100 mL respectively, this means that the value obtained from river water was 683 times higher than that obtained from the spring water. The groups of bacteria identified were total coliforms and Gram-negative bacilli made up of four genera, including the most predominant

Escherichia coli. As the values were higher than 0.00 MPN/100 mL, both types of water exceeded the recommended limit for total and fecal coliforms according to the WHO guidelines (WHO, 1997).

The C_f results showed 0 values for both types of samples, meaning that 100% removal of the total coliforms was found in both samples and can be attributed to appropriate disinfection pre-treatment of raw water (5). Also, high efficiency for removal of pathogenic microorganisms by the ultraviolet lamp (20) at AWP prototype was demonstrated.

Table 3. Total coliform of raw and water obtained from the AWP prototype.

Parameters	River water		Spring water		Units
	C_i	C_f	C_i	C_f	
Total coliforms	54,000±3%	0.00±0.00	79±2%	0.00±0.00	MPN/100 mL
Fecal coliforms	35,000±2%	0.00±0.00	Not detectable	0.00±0.00	MPN/100 mL

3.2. Chemical water quality

In Table 4 it is observed the average chemical parameters calculated from 3 times of sampling. The odor and flavor in both types of raw water were unpleasant, i.e., not suitable for human use. After the treatment with the AWP prototype, these parameters changed to nice, meaning the water samples comply the guidelines for drinking-water quality according to WHO and Mexican standards. The real color for river and spring water were 58.00±2% and 1.00±0.8% respectively, before percolation through the AWP prototype. After the treatment with the AWP prototype final concentrations were zero, fulfilling the guidelines of Mexican standards, since to the permitted value is 15 units (NOM-201-SSA1, 2002).

Complete removal of the organoleptic characteristics such as odor, flavor and color are due to the effective performance of adsorption columns with activated carbon materials (Figure 1, subsection 11-12).

In the case of the turbidity parameter the spring water C_i value was zero, therefore the C_f was the same. On the other hand, the reduction from 52.00 ±2% to 0 NTU was seen when the AWP prototype treatment was applied on the river water samples making only the AWP treated water below 1 NTU, the value that fulfilled the WHO guidelines (WHO, 1997).

The pH values as well were measured. The pH corresponding to C_i was 5±0.5% for both types of water and increased to 7.6±0.2% and 7.20±0.3% for river and spring water respectively. This was due to the clarification pre-treatment and proper functioning of adsorption columns (Figure 1, subsection 8-9). It means, the water treated with the AWP

prototype is the only one that satisfies the Mexican Official Standards (the permissible limits are from 6.5 to 8.5 units for pH (NOM-127-SSA1, 1994).

Figure 4 shows the removal percentage of chemical average parameters obtained by equation 1 and calculated within 6 times sampling. In this figure, it is shown the initial concentration (C_i) of total alkalinity, hardness and solids for river and spring water. As a first look, it's possible to realize that the river and spring water have high levels on those parameters. As the previous results, untreated waters were above the permissible limits. The recommended purified water limits for total alkalinity, hardness and solids were 300 mg/L, 200 mg/L and 500 mg/L, respectively. For example, the spring water was contaminated with high percentage of calcium (Ca^{2+}) and magnesium (Mg^{2+}) ion contents than river water. While, for both river and spring water the chloride and sulfate ions were 250 mg/L, below the permissible limits (NOM-127-SSA1, 1994).

Table 4. Main chemical contaminants of raw and water obtained from the AWP prototype.

Parameters	River water		Spring water		Units
	C_i	C_f	C_i	C_f	
Odor	Unpleasant	Nice	Unpleasant	Nice	--
Flavor	Unpleasant	Nice	Unpleasant	Nice	--
Real color	58.00±2%	0.00	1.00±0.8%	0.00	Units
Turbidity	52.00±2%	0.00	0.00	0.00	NTU
pH	5±0.5%	7.60±0.2%	5±0.5%	7.20±0.3%	Units

In Figure 5 it is shown the removal percentage (%R) and final concentration of heavy metals in zeolite ion exchange column (Figure 1, subsection 10) at AWP prototype, obtained by equation 2. The curves were fitted with the following mathematical equation by the exponential model:

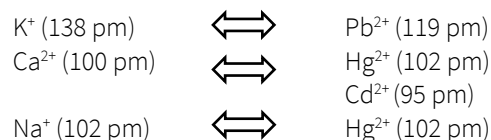
$$y = y_0 + Ae^{bx} \tag{2}$$

The removal rate of a cation in aqueous solution depends on the quantity exchanged in zeolite ion exchange column (10); as well on the function of the ion exchange. Thus, it was considered that under the same experimental conditions, the sample that has a higher capacity for a given ion exchange is one that exhibits the highest percentage of removal for that ion capacity (Erdem et al., 2004; Mihaly-Cozmuta et al., 2014).

In this figure, it is seen the removal percentage (circles) and final concentration (squares) against initial concentration for Pb^{2+} , Hg^{2+} , Cd^{2+} , and Cu^{2+} obtained from ICP-OES technique. It can

be seen that %R and C_f decrease as the initial metal concentration increases in aqueous solutions since zeolite has a maximum adsorption capacity and tends to become saturated at high concentrations. The %R varied from 87 to 99% for Pb^{2+} , 81 to 99% for Hg^{2+} , 77 to 98% for Cd^{2+} and 72 to 97% for Cu^{2+} .

Comparing the %R obtained from zeolite ion exchange column (10) for each metal, it is noted that the exchange selectivity in zeolite is $Pb^{2+} > Hg^{2+} > Cd^{2+} > Cu^{2+}$, i.e, for the natural zeolite the Pb^{2+} is exchanged in greater quantity than the metal Hg^{2+} and so for the metals Cd^{2+} and Cu^{2+} .



Where, pm means picometer and is equal to 0.001 nanometers (nm).

The literature indicates that in the case of metal cations and natural zeolites, the predominant mechanism is ion exchange. It can be assumed that the zeolite had a great amount of exchangeable K^+ ions, therefore, greater the exchange occurred with Pb^{2+} cation.

Final concentrations were 12.09 to 0.002 mg/L for Pb^{2+} , 18.7 to 0.002 mg/L for Hg^{2+} , 22.9 to 0.204 mg/L for Cd^{2+} and 28 to 0.5 mg/L for Cu^{2+} at initial concentration of 100 to 20 mg/L. The value of 20 mg/L of initial concentration are within permissible limit of purified water according to WHO guidelines that are 0.01 mg/L, 0.006 mg/L, 0.003 mg/L and 2.00 mg/L for Pb^{2+} , Hg^{2+} , Cd^{2+} , and Cu^{2+} respectively (Hersch, 2012).

These results indicate that the AWP prototype was designed to remove the main heavy metals described in Table 1 up to permissible limits from zeolite ion exchange column. The heavy metal uptake is attributed to different mechanisms of ion-exchange processes as well to the adsorption process. During the ion-exchange process, metal cations had to move through the pores of zeolite and channels of the lattice, which in turn replacing exchangeable cations (mainly Na^+ , Ca^{2+} and K^+). In this case the metal ion pickup could mainly be attributed to the ion-exchange reactions in the microporous minerals of the zeolite ion exchange column.

The maximum amount of metal ion exchanged per unit mass of the adsorbent represented by N_{max} (adsorbed, mg / zeolite, gr) was estimated using the least squares method by plotting the C/N ratio as a function of the equilibrium concentration C for each metal ion adjusted to a straight line with slope $1/N_{max}$ and ordered to the origin $1/KN_{max}$ for the Langmuir isotherm, using the following equation (Mihaly-Cozmuta et al., 2014):

$$\frac{C}{N} = \frac{C}{N_{max}} + \frac{1}{KN_{max}} \tag{3}$$

where, C is the concentration of metal ions at equilibrium, K is the Langmuir isotherm constant related to the enthalpy of adsorption. The values of N_{max} for each metal ion were: 1.785 mg/gr, 1.769 mg/gr, 1.753 mg/gr and 1.446 mg/gr for Pb^{2+} , Hg^{2+} , Cd^{2+} and Cu^{2+} respectively.

In Vivar's work (Vivar et al., 2017), it is confirmed that the treatment of water through SODIS (solar water disinfection) is not an effective method for elimination of bacteria and the efficiency depends on the season of the year and irradiance (W/m^2). A considerable amount of UV irradiation that

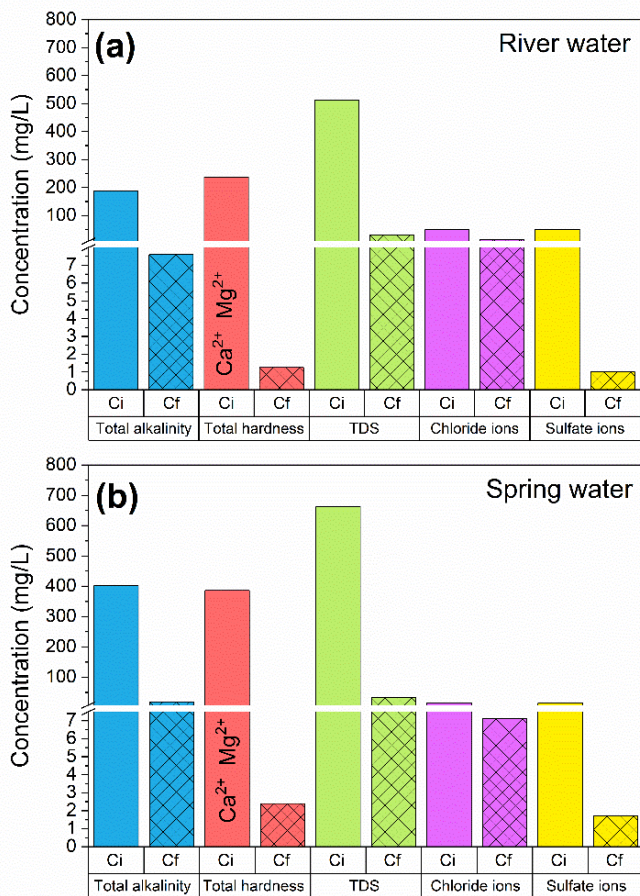


Figure 4. Concentration variation of chemical contaminants of raw water (C_i) and treated water (C_f) by the AWP prototype: a) river water and b) spring water.

This cation exchange can be attributed as the replacement of Na^+ , Ca^{2+} and K^+ exchangeable ions that constitute zeolite with the divalent cations of Pb^{2+} , Hg^{2+} , Cd^{2+} and Cu^{2+} . This isomorphous substitution is due to the similarity in their ionic radius that metal cations have with the exchangeable ions, the affinity of the dimensions in their cavities of zeolite makes one cation take the place of the other, by simple interaction between its chemical bonds. Due to the similarity between their ionic radius the replacement is concluded as follows (Shannon, 1976):

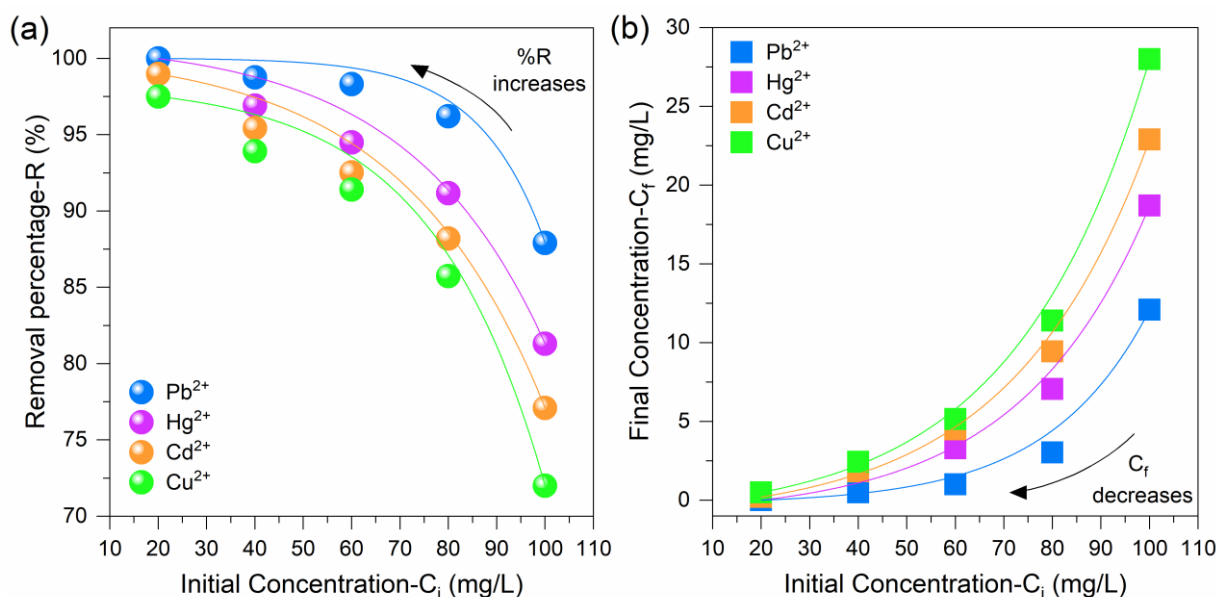


Figure 5. (a) Removal percentage (circles) and (b) final concentration (squares) of Pb^{2+} , Hg^{2+} , Cd^{2+} , and Cu^{2+} on zeolite ion exchange column as a function of the initial concentration.

arrives at the earth surface is UV-B (280-320 nm) and UV-A type (320-400 nm), this implies that it can break the simple DNA threads and destroy the cellular membrane of the microorganisms (Han et al., 2004).

Table 5. Summary of analytical results of raw and treated water samples by other similar systems.

Parameters	SODIS (Vivaret et al., 2017)		ECAS (Clayton et al., 2019)		AWP prototype (our work)	
	raw water	treated water	raw water	treated water	raw water	treated water
<i>E. coli</i>	1200 ± 45 CFU/100 mL	30 ± 3.0 CFU/100 mL	1.50 ± 0.71 CFU/100 mL	0.00 ± 0.00 CFU/100 mL	35,000 ± 2 MPN/100 mL	0.00 ± 0.00 MPN/100 mL
Total coliforms	11,000 ± 810 CFU/100 mL	270 ± 14 CFU/100 mL	12.0 ± 8.29 CFU/100 mL	0.00 ± 0.00 CFU/100 mL	54,000 ± 3 MPN/100 mL	0.00 ± 0.00 MPN/100 mL
Cadmium (Cd)	not evaluated	not evaluated	0.12 µg/L	0.10 µg/L (17%)	20 mg/L	0.204 mg/L (98.98%)
Copper (Cu)	not evaluated	not evaluated	0.01 mg/L	0.01 mg/L (0%)	20 mg/L	0.5 mg/L (97.5%)
Lead (Pb)	not evaluated	not evaluated	5.38 µg/L	0.62 µg/L (88%)	20 mg/L	0.002 mg/L (99.99%)

However, many of these microorganisms have a mechanism capable of repairing these effects. For this reason, the SODIS method can only eliminate 97.5% of *E. coli* and coliforms bacteria. In the ECAS method (electrochemically activated solutions) and in the AWP prototype the elimination was 100%. This is an important parameter, because according to the WHO guidelines the optimum value for water suitable for human consumption should be 0.00 MPN/100 mL or 0.00 CFU/100 mL. It should be mentioned that in our AWP prototype the concentration of the *E. coli* in the feed water was 30 times higher than that in SODIS.

In the case of heavy metals, it is observed that the ECAS method possesses a low removal efficiency of cadmium and copper, 17% and 0% respectively. While with the AWP prototype the removal, efficiencies are above 98% for cadmium, copper, and lead. This is because the ECAS method uses ultrafiltration (UF) membranes that work through a physical permeability mechanism that occurs by size separation through a membrane with pore size between 1 and 100 nm, which can retain colloidal matter and in suspension, as well as protozoa, bacteria, and most viruses (Arnal et al., 2009). Therefore, it was ideal for the elimination of macromolecules such as *E. coli* and coliform bacteria, but not for heavy metals that are smaller than 1 nm (Shannon, 1976).

The AWP prototype is proved to be capable of efficiently eliminating *E. coli* and coliform bacteria, as well as heavy metals, because it contains a UV irradiation stage that leads to

the cell death of microorganisms. Also, in addition to this a zeolite ion exchange column was added (Figure 1, subsection 10) the performance of this will be explained later.

Regarding the market, compared to commercial solar water purification systems distributed in e-commerce companies such as Alibaba and Indiamart, the market value of these products is between 300-1000 USD, for small systems of 15-20 L of water per day. For large systems with a production of more than 7,000 L/day the market value is between 18,000 and 25,000 USD, for example, the *H2Optima* solar water treatment plant. Our AWP prototype according to our business model is in the range of these values and would have a sale price of 900 USD (subject to change).

3.3. Chemical mechanisms in contaminants removal

Heavy metal removal was carried out in the zeolite ion exchange column (Figure 1, subsection 10) in the AWP prototype. The structure of zeolites (Figure 6a) forms a network of channels and cavities that allow easy penetration of molecules according to size, shape and polarity, leading to the adsorption and filtration of various substances that come into contact with zeolites (Abdel Rahim, 2017). One of the important mechanisms involved in the adsorption of toxins, such as heavy metals, is known as Cation Exchange Capacity (CEC), which is defined as the stoichiometric substitution of an equivalent ion in the solid phase for the equivalent of another ion in liquid phase (Petrus & Warchol, 2003). In the case of zeolites, it is considered as an intrinsic property since it is the product of the isomorphous substitution of the silicon atoms of its crystalline structure by other atoms. This substitution

occurs by tetravalent aluminum atoms, which produces a net negative charge in the structure that is compensated by cations external to them (Figure 6b). These cations are interchangeable and a manifestation of their nature of microporous crystalline structure since the dimensions of their cavities and of the cations that are exchanged determine the course of the process (Sherry, 2002). Figure 6a represents the ion exchange model for a clinoptilolite-K type zeolite with a high Si/Al ratio to show how different cations affect open pore cavities. As suggested in the literature, cationic charges affect the number of ion exchange during the exchange to maintain the valence balance of the zeolite (Figure 6b). According to the law of conservation of charge, each divalent cation (Pb^{2+} , Hg^{2+} , Cd^{2+} , and Cu^{2+}) consumes two monovalent sodium or potassium ion replacements (Na^+ and K^+) and vice versa (Sherry, 2002).

On the other hand, the elimination of bacteria such as *Escherichia coli* is carried out in the ultraviolet lamp (Figure 1, subsection 20) in our AWP prototype. Ultraviolet (UV) irradiation can be used to kill microorganisms, such as bacteria, fungi, fungal toxin viruses, and actinobacteria, with the sterilization efficiency determined by the wavelength of the applied light (Liu et al., 2019). The UV-C (200–280 nm) sterilization mechanism encompasses both physical and biochemical processes. When the microorganism absorbs ultraviolet light, a biochemical process of formation of pyrimidine dimers and thymine dimers occurs, which may interfere with the microorganism's DNA and eventually leads to cell death (Petrus & Warchol, 2003), this mechanism is shown in Figure 6c.

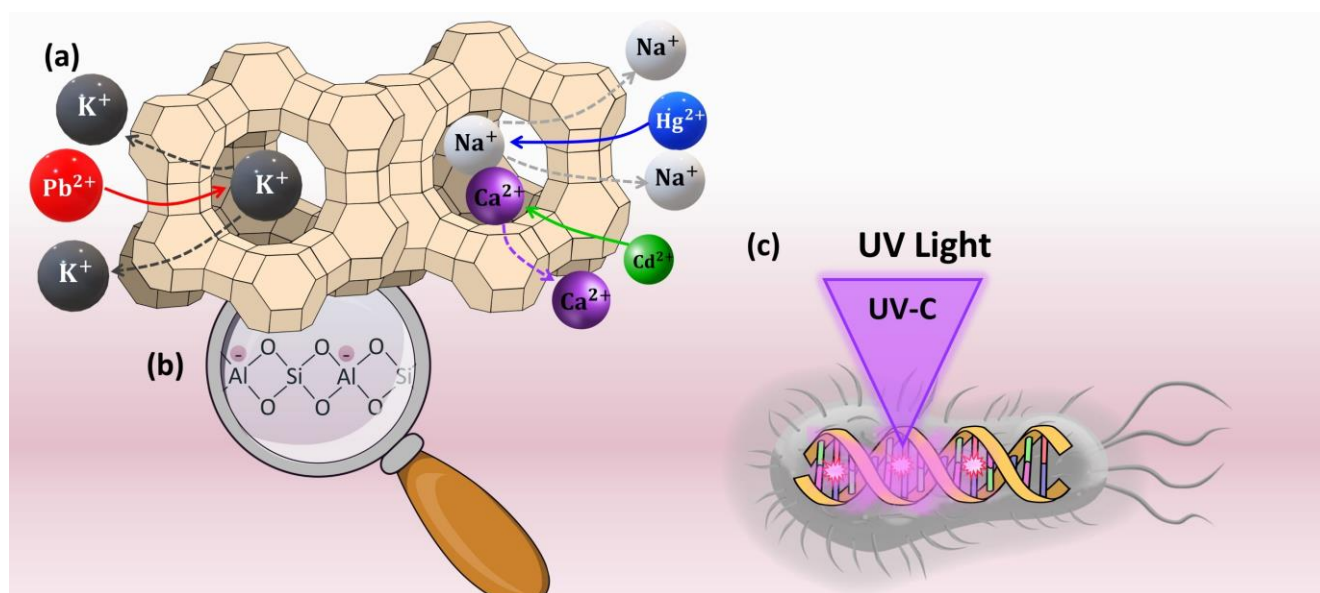


Figure 6. (a) Model of different cation exchanges in the structure of a zeolite; (b) ion exchange scheme on the surface of a zeolite; (c) scheme for elimination of microorganisms by UV light.

In this work it is presented a new concept of portable water purifier to produce clean water. The aim of the study was to satisfy the need for clean water in places where they do not have access to this service or to the electricity grid, for example at rural and natural disaster areas. The study demonstrated the design, and it was discussed its performance in this article. The AWP showed autonomy by using an autonomous photovoltaic system that uses solar energy for its operation, the prototype was designed to operate up to 8 hours a day and generates a water flow of 112 L/day and the capacity of batteries gave a prolonged autonomy (4 days) to ensure the uninterrupted operation of the system.

It showed high efficiency on removing microbiological and chemical agents (up to 50-100%) such as total coliforms, fecal coliforms, total alkalinity, total hardness, total solids, chloride, sulfate and heavy metals. For chemical agents the decrease was from 70 to 99% after AWP treatment, and all the chemical and microbiological analyses showed total removal of *E. coli* and coliforms were achieved. The AWP prototype integrated different mechanisms of adsorption, ion exchange, reverse osmosis, ultraviolet radiation, disinfection and clarification.

The design of purification steps such as microfiltration, ultrafiltration, nanofiltration, reverse osmosis, disinfection, clarification and ion exchange processes allowed to obtain an extensive range of removal of contaminants and heavy metals compared to other purifiers, for that reason this novel prototype can remove toxic chemical contaminants such as heavy metals. The results showed that the ion exchange column evaluation with zeolite could be used effectively for the removal of heavy metals from raw water. The evaluation on raw natural waters reveals that this prototype is suitable and appropriate to treat water from different sources, with high concentrations and different types of contaminants. Resulting in clean, healthy, and safe water for human consumption, with good taste, odor and color.

Conflict of interest

The authors have no conflict of interest to declare.

Acknowledgments

The authors would like to thank the technical support received from Rocio Meza-Gordillo for ICP-OES characterization, Alison Ruiz-Suárez, and Erick Alejandro Hernández-Domínguez for their support with the analysis of heavy metals. Dulce K. Becerra-Paniagua acknowledges Consejo Nacional de Ciencia y Tecnología (CONACyT-Mexico) for her PhD scholarship and Universidad de Ciencias y Artes de Chiapas. Araceli Hernández thanks DGAPA-UNAM for the financial support received for her postdoctoral fellowship.

Financing

The authors received no specific funding for this work.

References

- Abdel-Rahim, M. M. (2017). Sustainable use of natural zeolites in aquaculture: a short review. *Oceanography & Fisheries*, 2(4), 1-5. <https://doi.org/10.19080/foaj.2017.02.555593>
- Alghoul, M. A., Poovanaesvaran, P., Mohammed, M. H., Fadhil, A. M., Muftah, A. F., Alkilani, M. M., & Sopian, K. (2016). Design and experimental performance of brackish water reverse osmosis desalination unit powered by 2 kW photovoltaic system. *Renewable Energy*, 93, 101-114. <https://doi.org/10.1016/j.renene.2016.02.015>
- Aragonés-Beltrán, P., Mendoza-Roca, J. A., Bes-Piá, A., García-Melón, M., & Parra-Ruiz, E. (2009). Application of multicriteria decision analysis to jar-test results for chemicals selection in the physical-chemical treatment of textile wastewater. *Journal of Hazardous Materials*, 164(1), 288-295. <https://doi.org/10.1016/j.jhazmat.2008.08.046>
- Arnal, J. M., Garcia-Fayos, B., Verdu, G., & Lora, J. (2009). Ultrafiltration as an alternative membrane technology to obtain safe drinking water from surface water: 10 years of experience on the scope of the AQUAPOT project. *Desalination*, 248(1-3), 34-41. <https://doi.org/10.1016/j.desal.2008.05.035>
- Clayton, G. E., Thorn, R. M. S., & Reynolds, D. M. (2019). Development of a novel off-grid drinking water production system integrating electrochemically activated solutions and ultrafiltration membranes. *Journal of Water Process Engineering*, 30, 100480. <https://doi.org/10.1016/j.jwpe.2017.08.018>
- Elboughdiri, N. (2020). The use of natural zeolite to remove heavy metals Cu (II), Pb (II) and Cd (II), from industrial wastewater. *Cogent Engineering*, 7(1). <https://doi.org/10.1080/23311916.2020.1782623>
- Erdem, E., Karapinar, N., & Donat, R. (2004). The removal of heavy metal cations by natural zeolites. *Journal of Colloid and Interface Science*, 280(2), 309-314. <https://doi.org/10.1016/j.jcis.2004.08.028>
- Fernandez-Ibanez, P., Polo-López, M. I., Malato, S., Wadhwa, S., Hamilton, J. W. J., Dunlop, P. S. M., ... & Byrne, J. A. (2015). Solar photocatalytic disinfection of water using titanium dioxide graphene composites. *Chemical Engineering Journal*, 261, 36-44. <https://doi.org/10.1016/j.cej.2014.06.089>

- Flachsbarth, I., Willaarts, B., Xie, H., Pitois, G., Mueller, N. D., Ringler, C., & Garrido, A. (2015). The Role of Latin America's Land and Water Resources for Global Food Security: Environmental Trade-Offs of Future Food Production Pathways. *PLOS ONE*, 10(1), e0116733. <https://doi.org/10.1371/journal.pone.0116733>
- Gutierrez-Jimenez, J. (2014). Evaluation of A Point-Of Use Water Purification System (Llaveoz) in a Rural Setting of Chiapas, Mexico. *Journal of Microbiology & Experimentation*, 1(3). <https://doi.org/10.15406/jmen.2014.01.00015>
- Gutiérrez-Jiménez, J., Luna-Cázares, L. M., Martínez-de la Cruz, L., Aquino-López, J. A. D., Sandoval-Gómez, D., León-Ortiz, A. T., ... & Vidal, J. E. (2019). Children from a rural region in The Chiapas Highlands, Mexico, show an increased risk of stunting and intestinal parasitoses when compared with urban children. *Boletín médico del Hospital Infantil de México*, 76(1), 18-26. <https://doi.org/10.24875/BMHIM.18000069>
- Han, J., Colditz, G. A., Samson, L. D., & Hunter, D. J. (2004). Polymorphisms in DNA Double-Strand Break Repair Genes and Skin Cancer Risk. *Cancer Research*, 64(9), 3009–3013. <https://doi.org/10.1158/0008-5472.CAN-04-0246>
- Holtman, G. A., Haldenwang, R., & Welz, P. J. (2018). Biological sand filter system treating winery effluent for effective reduction in organic load and pH neutralisation. *Journal of Water Process Engineering*, 25, 118–127. <https://doi.org/10.1016/j.jwpe.2018.07.008>
- Jaishankar, M., Tseten, T., Anbalagan, N., Mathew, B. B., & Beeregowda, K. N. (2014). Toxicity, mechanism and health effects of some heavy metals. *Interdisciplinary Toxicology*, 7(2), 60–72. <https://doi.org/10.2478/intox-2014-0009>
- Kohn, T., Mattle, M. J., Minella, M., & Vione, D. (2016). A modeling approach to estimate the solar disinfection of viral indicator organisms in waste stabilization ponds and surface waters. *Water Research*, 88, 912–922. <https://doi.org/10.1016/j.watres.2015.11.022>
- Liu, C. Y., Tseng, C. H., Wang, H. C., Dai, C. F., & Shih, Y. H. (2019). The study of an ultraviolet radiation technique for removal of the indoor air volatile organic compounds and bioaerosol. *International Journal of Environmental Research and Public Health*, 16(14), 2557. <https://doi.org/10.3390/ijerph16142557>
- Luque, A., & Hegedus, S. (2011). *Handbook of photovoltaic science and engineering*. John Wiley & Sons. <https://doi.org/10.1002/0470014008>
- Marazzato, M., Aleandri, M., Massaro, M. R., Vitanza, L., Conte, A. L., Conte, M. P., ... & Longhi, C. (2020). Escherichia coli strains of chicken and human origin: Characterization of antibiotic and heavy-metal resistance profiles, phylogenetic grouping, and presence of virulence genetic markers. *Research in Veterinary Science*, 132, 150-155. <https://doi.org/10.1016/j.rvsc.2020.06.012>
- Matsumoto, Y., Valdés, M., Urbano, J. A., Kobayashi, T., López, G., & Peña, R. (2014). Global Solar Irradiation in North Mexico City and Some Comparisons with the South. *Energy Procedia*, 57, 1179–1188. <https://doi.org/10.1016/j.egypro.2014.10.105>
- Mekonnen, M., Pahlow, M., Aldaya, M., Zarate, E., & Hoekstra, A. (2015). Sustainability, Efficiency and Equitability of Water Consumption and Pollution in Latin America and the Caribbean. *Sustainability*, 7(2), 2086–2112. <https://doi.org/10.3390/su7022086>
- Mihaly-Cozmuta, L., Mihaly-Cozmuta, A., Peter, A., Nicula, C., Tutu, H., Silipas, D., & Indrea, E. (2014). Adsorption of heavy metal cations by Na-clinoptilolite: Equilibrium and selectivity studies. *Journal of Environmental Management*, 137, 69–80. <https://doi.org/10.1016/j.jenvman.2014.02.007>
- Murray, A. L., Napotnik, J. A., Rayner, J. S., Mendoza, A., Mitro, B., Norville, J., ... & Lantagne, D. S. (2020). Evaluation of consistent use, barriers to use, and microbiological effectiveness of three prototype household water treatment technologies in Haiti, Kenya, and Nicaragua. *Science of the Total Environment*, 718, 134685. <https://doi.org/10.1016/j.scitotenv.2019.134685>
- NOM-127-SSA1-1994. (1994). MODIFICACION a la Norma Oficial Mexicana [NOM-127-SSA1-1994] Salud ambiental. *Agua para uso y consumo humano*. Límites permisibles de calidad y tratamientos a que debe someterse el agua para su potabilización. <http://www.salud.gob.mx/unidades/cdi/nom/m127ssa14.html>
- Norma Oficial Mexicana [NOM-201-SSA1-2002] (2002). Productos y servicios. *Agua y hielo para consumo humano, envasados y a granel*. Especificaciones sanitarias. <http://www.salud.gob.mx/unidades/cdi/nom/201ssa12.html>
- Statistics on Water in Mexico. (2017). *National Water Commission*. 1-192.
- Ochoa-Gutiérrez, K. S., Tabares-Aguilar, E., Mueses, M. Á., Machuca-Martínez, F., & Li Puma, G. (2018). A Novel Prototype Offset Multi Tubular Photoreactor (OMTP) for solar photocatalytic degradation of water contaminants. *Chemical Engineering Journal*, 341, 628–638. <https://doi.org/10.1016/j.cej.2018.02.068>

- Pan American Health Organization (PAHO). (2017). *Health in the Americas+*, 2017 Edition. Summary Regional Outlook and Country Profiles.
<https://iris.paho.org/handle/10665.2/34469>
- Pan American Health Organization (PAHO) / World Health Organization (WHO). (2019). [Nearly 16 million people still practice open defecation in Latin America and the Caribbean.](#)
- Parsa, S. M., Rahbar, A., Koleini, M. H., Javadi, Y. D., Afrand, M., Rostami, S., & Amidpour, M. (2020). First approach on nanofluid-based solar still in high altitude for water desalination and solar water disinfection (SODIS). *Desalination*, 491, 114592.
<https://doi.org/10.1016/j.desal.2020.114592>
- Peng, W., Maleki, A., Rosen, M. A., & Azarikhah, P. (2018). Optimization of a hybrid system for solar-wind-based water desalination by reverse osmosis: Comparison of approaches. *Desalination*, 442, 16–31.
<https://doi.org/10.1016/j.desal.2018.03.021>
- Pérez-Denicia, E., Fernández-Luqueño, F., Vilariño-Ayala, D., Montañó-Zetina, L. M., & Maldonado-López, L. A. (2017). Renewable energy sources for electricity generation in Mexico: A review. *Renewable and Sustainable Energy Reviews*, 78, 597-613.
<https://doi.org/10.1016/j.rser.2017.05.009>
- Petrus, R., & Warchot, J. (2003). Ion exchange equilibria between clinoptilolite and aqueous solutions of $\text{Na}^+/\text{Cu}^{2+}$, $\text{Na}^+/\text{Cd}^{2+}$ and $\text{Na}^+/\text{Pb}^{2+}$. *Microporous and Mesoporous Materials*, 61(1–3), 137–146.
[https://doi.org/10.1016/S1387-1811\(03\)00361-5](https://doi.org/10.1016/S1387-1811(03)00361-5)
- Qin, L., Wang, Y., Vivar, M., Huang, Q., Zhu, L., Fuentes, M., & Wang, Z. (2015). Comparison of photovoltaic and photocatalytic performance of non-concentrating and V-trough SOLWAT (solar water purification and renewable electricity generation) systems for water purification. *Energy*, 85, 251–260.
<https://doi.org/10.1016/j.energy.2015.03.106>
- REdataexplorer (2022).
<https://www.re-explorer.org/re-data-explorer/subscribe>
- Rice, E. W., Baird, R. B., & Eaton, A. D. (2017). [Standard Methods for the Examination of Water and Wastewater ed-23rd. American Public Health Association \(APHA\), American Water Works Association \(AWWA\) and Water Environment Federation \(WEF\), Washington DC.](#)
- Shaharoon, B., Al-Ismaïly, S., Al-Mayahi, A., Al-Harrasi, N., Al-Kindi, R., Al-Sulaimi, A., ... & Al-Abri, M. (2019). The role of urbanization in soil and groundwater contamination by heavy metals and pathogenic bacteria: A case study from Oman. *Heliyon*, 5(5), e01771.
<https://doi.org/10.1016/j.heliyon.2019.e01771>
- Shannon, R. D. (1976). Revised effective ionic radii and systematic studies of interatomic distances in halides and chalcogenides. *Acta Crystallographica Section A*, 32(5), 751–767.
<https://doi.org/10.1107/S0567739476001551>
- Sherry, H. S. (2002). The Ion-Exchange Properties of Zeolites. I. Univalent Ion Exchange in Synthetic Faujasite. *Journal of Physical Chemistry*, 70(4), 1158–1168.
<https://doi.org/10.1021/J100876A031>
- Stevens, G., Dias, R. H., Thomas, K. J. A., Rivera, J. A., Carvalho, N., Barquera, S., ... & Ezzati, M. (2008). Characterizing the epidemiological transition in Mexico: national and subnational burden of diseases, injuries, and risk factors. *PLoS medicine*, 5(6), e125.
<https://doi.org/10.1371/journal.pmed.0050125>
- World Health Organization & United Nations Children's Fund (UNICEF). (2015). *Progress on sanitation and drinking water: 2015 update and MDG assessment.*
<https://www.who.int/publications/i/item/9789241509145>
- World Health Organization & United Nations Children's Fund (UNICEF). (2017a).
<https://www.who.int/news-room/fact-sheets/detail/diarrhoeal-disease>
- World Health Organization / United Nations Children's Fund (UNICEF). (2017b). [Progress on drinking water, sanitation and hygiene.](#)
- World Health Organization & United Nations Children's Fund (UNICEF). (2019). *Progress on household drinking water, sanitation, and hygiene 2000-2017: special focus on inequalities.* World Health Organization.
<https://apps.who.int/iris/handle/10665/329370>
- Valdes-Barrón, M., Riveros-Rosas, D., Arancibia-Bulnes, C. A., & Bonifaz, R. (2014). The Solar Resource Assessment in Mexico: State of the Art. *Energy Procedia*, 57, 1299–1308.
<https://doi.org/10.1016/j.egypro.2014.10.120>

Vivar, M., Fuentes, M., Dodd, N., Scott, J., Skryabin, I., & Srithar, K. (2012). First lab-scale experimental results from a hybrid solar water purification and photovoltaic system. *Solar Energy Materials and Solar Cells*, 98, 260–266.

<https://doi.org/10.1016/j.solmat.2011.11.012>

Vivar, M., Pichel, N., & Fuentes, M. (2017). Solar disinfection of natural river water with low microbiological content (10–103CFU/100 ml) and evaluation of the thermal contribution to water purification. *Solar Energy*, 141, 1–10.

<https://doi.org/10.1016/j.solener.2016.11.019>

Wang, Y., Jin, Y., Huang, Q., Zhu, L., Vivar, M., Qin, L., Sun, Y., Cui, Y., & Cui, L. (2016). Photovoltaic and disinfection performance study of a hybrid photovoltaic-solar water disinfection system. *Energy*, 106, 757–764.

<https://doi.org/10.1016/j.energy.2016.03.112>

World Health Organization (WHO). (1997). *Guidelines for drinking-water quality*. Vol. 3, Surveillance and control of community supplies. Vol. 3, Vigilancia y control de los abastecimientos de agua a la comunidad, 2nd ed. World Health Organization.

<https://apps.who.int/iris/handle/10665/42002>

Herschy R. W. (2012). Water Quality for Drinking: WHO Guidelines. In: Bengtsson L., Herschy R.W., Fairbridge R.W. (eds) *Encyclopedia of Lakes and Reservoirs. Encyclopedia of Earth Sciences Series*. Springer, Dordrecht.

https://doi.org/10.1007/978-1-4020-4410-6_184

Wu, M. J., Bak, T., O'Doherty, P. J., Moffitt, M. C., Nowotny, J., Bailey, T. D., & Kersaitis, C. (2014). Photocatalysis of Titanium Dioxide for Water Disinfection: Challenges and Future Perspectives. *International Journal of Photochemistry*, 2014, 1–9.

<https://doi.org/10.1155/2014/973484>